Mode structure and the noise performance of a gain-guided amplifier

J. G. Wessel, P. R. Battle,* and J. L. Carlsten
Physics Department, Montana State University, Bozeman, Montana 59717
(Received 2 December 1993)

The spatial structure of a gain-guided amplifier is naturally described by a set of nonorthogonal modes. We present an analysis of the mode structure of an amplifier with a focused Gaussian gain. It is found that the modes are spatially narrower and have a different radius of curvature than the corresponding free-space modes. A calculation of the signal-to-noise ratio shows that the spatial structure of the input field has a significant effect on the amplifier noise performance.

PACS number(s): 42.60.Da, 42.65.Dr

I. INTRODUCTION

To solve the three-dimensional wave equation describing growth of a field in gain-guided amplifier (GGA) it is convenient to write the amplified field as a sum of nonorthogonal modes [1–6]. The nonorthogonal modes can be considered the natural modes of the system because they are the eigenmodes of the non-Hermitian wave equation describing the amplified field and, for the case of a long amplifier, only one nonorthogonal mode is significantly populated [1,6]. This is in contrast to the many orthogonal modes needed to describe the amplified field [7]. A nonorthogonal mode basis is a convenient basis to employ when describing systems whose wave equations or boundary conditions are non-Hermitian. Examples of such systems are gain-guided amplifiers and unstable resonators [2].

As a consequence of the nonorthogonality of the modes, the amount of noise effectively seeding a mode can be larger than the usual quantum limit [8]. To account for spontaneous emission in a power orthogonal basis, one noise photon is considered to seed each mode [1–3,9–11]. On the other hand, when a nonorthogonal mode basis is employed the spontaneous emission into different modes is correlated. Therefore the amount of spontaneous emission effectively seeding each mode can be significantly larger than one photon. Some authors have labeled this phenomena "excess spontaneous emission," but following Haus and Kawakami [1] we prefer to call it "excess noise." It has been shown, however, that the performance of an amplifier is not necessarily degraded by the excess noise [1,2]. An important measure of amplifier performance, the signal-to-noise ratio (SNR), can still be at the quantum limit if an input signal has the proper spatial structure. Modes with the proper structure to maximize the SNR turn out to be the eigenmodes of the Hermitian adjoint of the wave equation describing the GGA and as such are called adjoint modes.

Many insightful and informative papers have already been published on the subject of excess noise and nonorthogonal modes of GGA's [1–6]. The emphasis in most of these articles was to either find an expression for the output power from the amplifier or analyze the implications of the excess noise. While almost all of the above-mentioned papers present a mathematical derivation of the nonorthogonal modes, few discuss the structure of the modes. In this paper, plots of the amplitude and phase of these modes are presented and compared to the usual orthogonal modes. Although we will concentrate on the nonorthogonal modes for an amplifier with focused Gaussian gain, much of the discussion is applicable to other gain profiles.

The issue of coupling into a gain-guided amplifier is also addressed. It is theoretically well established that the amplifier performance is maximized if the input signal is an adjoint mode [1,2]. However, for a Gaussian gain profile, it is experimentally nontrivial to construct an adjoint mode. We therefore discuss the SNR of an amplifier for inputs which are experimentally more convenient: a nonorthogonal mode input and a simple Gaussian input. This knowledge of predicted amplifier performance is crucial for efficient use of GGA's.

This paper is organized as follows. In Sec. II a brief review of the nonorthogonal mode theory for a focused Gaussian gain amplifier is presented. In Sec. III we analyze the radius of curvature and the waists of both the nonorthogonal modes and the adjoint modes. Discussion of amplifier performance for adjoint mode, nonorthogonal mode, and Gaussian mode inputs is presented in Sec. IV. Section V is the conclusion.

II. THEORY

To model theoretically the growth from spontaneous emission in an amplifier with focused gain we start with Maxwell's wave equation. The steady-state time-averaged, paraxial wave equation for a slowly varying electric field traveling in the positive z direction is [1,3,6]

$$[\nabla_T^2 - 2ik\partial_z + ikg(z,\mathbf{r}_T)]\hat{E}^{(-)}(z,\mathbf{r}_T) = -k^2 4\pi \hat{P}^{\dagger}_{\rm sp}(z,\mathbf{r}_T)\ , \quad (1)$$

*Present address: Physics Branch, Code 5640, Optical Sciences Division, Naval Research Laboratory, Washington, D.C. 20375.

where $\nabla_T^2=\partial_x^2+\partial_y^2$, $\mathbf{r}_T=x\hat{\mathbf{x}}+y\hat{\mathbf{y}}$, and $k=\omega/c$. $g(z,\mathbf{r}_T)$ represents the gain profile, due to a pump laser, which we take to be proportional to a focused Gaussian [7], i.e.,

$$g(z,\mathbf{r}_T)=\frac{4G\exp[-2r^2/\omega_g^2(z)]}{k_g\omega_g^2(z)}\ , \tag{2}$$

where $\omega_g^2(z)=\omega_0^2[1+(z/z_0)^2]$ is the transverse radius (squared), $r=|\mathbf{r}_T|$, z_0 is the Rayleigh range, and G is a dimensionless gain coefficient. Note that since the gain profile is a focused Gaussian, the diffraction of the pump beam is incorporated into Eq. (1). The transverse Laplacian in Eq. (1) accounts for the diffraction of the amplified field. To account for spontaneous emission the time-averaged quantum Langevin operator $\hat{P}_{\rm sp}^{\dagger}(z,\mathbf{r}_T)$, which represents the quantum fluctuations in the polarization of the medium, is included [3,12].

The field and polarization operators in Eq. (1) represent time-averaged quantities and thus are independent of time. In the Appendix, we show how the Maxwell-Bloch equations of stimulated Raman scattering can be reduced to this form. It is important to note, however, that Eq. (1) is a general expression describing many types of GGA's [2–4].

The detailed solution to Eq. (1) has already been presented elsewhere [6] and is not duplicated here. However, for the sake of continuity a short summary of the solution is presented. To solve Eq. (1), the amplified field is expanded into a set of nonorthogonal modes

$$\hat{E}^{(-)}(z,\mathbf{r}_T)=\left[\frac{2\pi\Delta\nu\hbar\omega}{c}\right]^{1/2}\sum_{n,l}\hat{a}_n^{l\dagger}(z)\Phi_n^l(z,\mathbf{r}_T)\ , \tag{3}$$

where $\hat{a}_n^{l\dagger}(z)$ is a generalized creation operator [3,6,13] for the photons in the nonorthogonal mode $\Phi_n^l(z,\mathbf{r}_T)$ and $\Delta\nu$ is the amplifier bandwidth. The modes $\{\Phi_n^l(z,\mathbf{r}_T)\}$ are not arbitrary; rather they are chosen to satisfy the eigenvalue equation

$$[\nabla_T^2-2ik\partial_z+ikg(z,\mathbf{r}_T)]\Phi_n^l(z,\mathbf{r}_T)=\lambda_n^l\frac{4ik}{k_g\omega_g^2(z)}\Phi_n^l(z,\mathbf{r}_T)\ , \tag{4}$$

where λ_n^l is the eigenvalue associated with the mode $\Phi_n^l(z,\mathbf{r}_T)$. The indices n and l correspond to the radial and angular degrees of freedom, respectively. Because the modes $\Phi_n^l(z,\mathbf{r}_T)$ are eigenmodes of a non-Hermitian operator [the presence of the gain term in Eq. (4) makes it non-Hermitian] they are not guaranteed to form a complete set. In addition, the modes are not orthogonal to each other in the usual manner. Instead, one finds [14]

$$B_{n,m}^l=\int d^2r_T\Phi_m^{l*}(z,\mathbf{r}_T)\Phi_n^l(z,\mathbf{r}_T)\neq\delta_{m,n}\ . \tag{5}$$

The quantity $(B_{n,n}^l)^2$ is referred to as the excess spontaneous emission or Petermann factor for the mode $\Phi_n^l(z,\mathbf{r}_T)$ and is greater than or equal to unity [8].

There does, however, exist an orthogonality relationship with the set of adjoint modes $\{\Psi_n^l(z,\mathbf{r}_T)\}$. The adjoint modes are solutions to the differential equation formed by taking the Hermitian adjoint of Eq. (4). The biorthogonality relationship is expressed as

$$\int d^2r_T\Psi_m^{k*}(z,\mathbf{r}_T)\Phi_n^l(z,\mathbf{r}_T)=\delta_{m,n}\delta_{k,l}\ . \tag{6}$$

Physically, the adjoint modes correspond to the nonorthogonal modes propagating backward through the amplifier [2,3].

To solve for the total power in the amplified field, the normally ordered product of the field is integrated over the transverse coordinates:

$$P=\frac{c}{2\pi}\int d^2r_T\langle\hat{E}^{(-)}(z,\mathbf{r}_T)\hat{E}^{(+)}(z,\mathbf{r}_T)\rangle$$
$$=\Delta\nu\hbar\omega\sum_{n,p,k,l}\langle\hat{a}_n^{k\dagger}(z)\hat{a}_p^l(z)\rangle\int d^2r_T\Phi_n^k(z,\mathbf{r}_T)\Phi_p^{l*}(z,\mathbf{r}_T)\ . \tag{7}$$

Note that since the modes are not orthogonal the cross terms do not vanish. The value of the correlation $\langle\hat{a}_n^{l\dagger}(z)\hat{a}_p^l(z)\rangle$ is obtained by modeling the amplifier as a completely inverted two-level system. This model, though simple, has been used to describe a wide range of amplifiers from the Raman amplifier to a single-pass x-ray laser [4]. The details of these calculations can be found in previous work [6]. The total power contained in the field at position z is

$$P=\Delta\nu\hbar\omega\sum_l\sum_{n,p}B_{p,n}^l(B_{p,n}^l\{\exp[(\lambda_n^l+\lambda_p^{l*})(\theta-\theta_i)]-1\}+\langle\hat{a}_n^{l\dagger}(\theta_i)\hat{a}_p^l(\theta_i)\rangle\times\exp[(\lambda_n^l+\lambda_p^{l*})(\theta-\theta_i)])\ , \tag{8}$$

where the transformation $\theta=\tan^{-1}(z/z_0)$ [7], which has the effect of folding out the focused nature of the fields, has been made and θ_i locates the entrance to the amplifier. The correlation $\langle\hat{a}_n^{l\dagger}(\theta_i)\hat{a}_p^l(\theta_i)\rangle$ is related to the external signal input into the amplifier. Note that we have assumed the external input has the same bandwidth as the amplifier. The expression for total output power has two distinct contributions: The first corresponds to amplified spontaneous emission, while the second represents the amplified input into the amplifier.

The utility of the nonorthogonal mode expansion is most evident when the expression for power, Eq. (8), is dominated by a single nonorthogonal mode, as is the case for a long, high gain amplifier [1,6,15]. In this case only the lowest order mode ($l=n=0$) has significant population, and thus the total power can be written

$$P\approx\Delta\nu\hbar\omega[B^2+B\langle\hat{a}^{\dagger}(\theta_i)\hat{a}(\theta_i)\rangle]\exp[2\,\mathrm{Re}(\lambda)(\theta-\theta_i)]\ , \tag{9}$$

where all subscripts and superscripts on B, $\hat{a}^{\dagger}(\theta_i)$, and λ have been dropped since they will be zero, unless otherwise noted, for the remainder of this paper.

When there is no external input into the amplifier [$\langle\hat{a}^{\dagger}(\theta_i)\hat{a}(\theta_i)\rangle=0$], the output is due to amplified spontaneous emission only. In this case, Eq. (9) shows that the effective noise input, into $\Phi(z,\mathbf{r}_T)$, due to gain guiding, is B^2 (>1) photons. Therefore, since the effective input into the orthogonal modes describing an inverted,

two-level amplifier operating at the quantum limit is one photon [1,2,9–11], $\Phi(z,\mathbf{r}_T)$ is said to have excess noise [1]. In Sec. IV it is shown that gain guiding can have a significant effect on the SNR of an amplifier.

III. DISCUSSION OF MODES

In this section the spatial structure of the nonorthogonal modes of a focused GGA is explored. For simplicity the spatial structure of only the lowest-order nonorthogonal mode $\Phi(z,\mathbf{r}_T)$ is examined. Higher-order nonorthogonal modes are expected to have features similar to $\Phi(z,\mathbf{r}_T)$ and thus will not be discussed.

To solve Eq. (4), it is convenient to write the nonorthogonal modes as linear combinations of the free-space, or Gauss-Laguerre, modes, which are denoted by $U_n^l(z,\mathbf{r}_T)$ [or simply $U(z,\mathbf{r}_T)$ when $n=l=0$] [6,7]. The $\{U_n^l(z,\mathbf{r}_T)\}$ are solutions to Eq. (4) when both $g(z,\mathbf{r}_T)$ and λ_n^l are zero. The free-space modes used in the linear combination to represent $\Phi(z,\mathbf{r}_T)$ are chosen to have the same confocal parameter as the gain medium. The coefficients of expansion are functions of the amplifier gain G, thus the shape of $\Phi(z,\mathbf{r}_T)$ is also a function of the gain. At low gains $\Phi(z,\mathbf{r}_T)\approx U(z,\mathbf{r}_T)$, where $U(z,\mathbf{r}_T)$ is the usual focused Gaussian, but as the gain increases, $\Phi(z,\mathbf{r}_T)$ becomes spatially narrower than $U(z,\mathbf{r}_T)$. Therefore many free-space modes must be added together to represent the narrowed nonorthogonal mode. This narrowing is known as transverse gain narrowing and can be understood in the following way: since the gain is largest on axis the mode grows more rapidly on axis than it does off axis. A direct measurement of the narrowing has been carried out by LaSala, Deacon, and Madey [16] for a free-electron laser and by Duncan *et al.* for a Raman amplifier [17].

An example of the transverse narrowing is shown in Fig. 1 where we plot the intensity distribution of $\Phi(z,\mathbf{r}_T)$, with $U(z,\mathbf{r}_T)$ included for reference, as a function of $r/\omega_g(z)$. Since $r/\omega_g(z)$ is a function of z, Fig. 1 is valid everywhere in the gain region. It is interesting to note that $\Phi(z,\mathbf{r}_T)$ can be narrower than $U(z,\mathbf{r}_T)$, yet both modes diffract at the same rate. The plot was generated using a gain of $G=3$, which corresponds to the maximum gain used in previous Raman scattering experiments in which gain-guiding effects were evident [6].

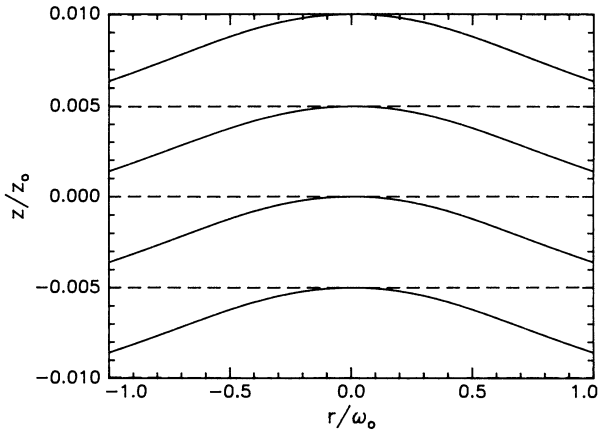

FIG. 2. Wave fronts for both the dominant nonorthogonal mode (solid line) and the lowest-order free-space mode (dashed line) in the region near focus. The curved wave fronts of the nonorthogonal mode indicate that gain guiding is occurring.

It is also found that gain guiding causes the nonorthogonal modes to have a radius of curvature that can be significantly different than that of the free-space modes. In Fig. 2 an example of wave-front distortion due to gain guiding is shown. The wave fronts (lines of constant phase) are plotted for both $\Phi(z,\mathbf{r}_T)$ (solid line) and $U(z,\mathbf{r}_T)$ (dashed line) in the region near focus where $|z/z_0|\ll 1$ [18]. In this region the wave fronts of $U(z,\mathbf{r}_T)$ [and $\Phi(z,\mathbf{r}_T)$ for $G\to 0$] are essentially flat. Therefore any deviation of $\Phi(z,\mathbf{r}_T)$'s wave fronts from flatness is an indication that gain guiding is occurring.

While Fig. 2 shows the nonorthogonal modes only in the region near focus where $|z/z_0|\ll 1$, Fig. 3 shows the

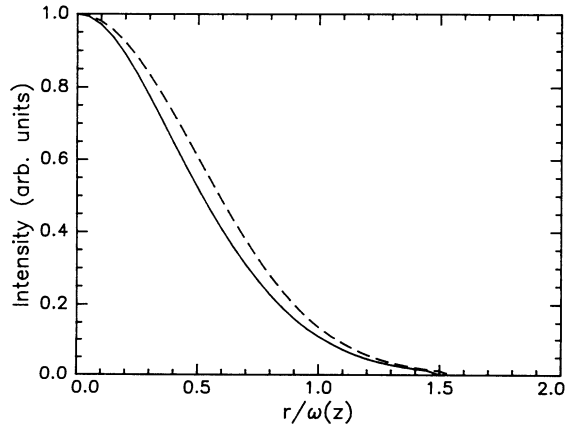

FIG. 1. Transverse intensity distribution of the dominant nonorthogonal mode (solid line) and lowest-order free-space mode (dashed line). The nonorthogonal mode is narrower as a result of transverse gain narrowing.

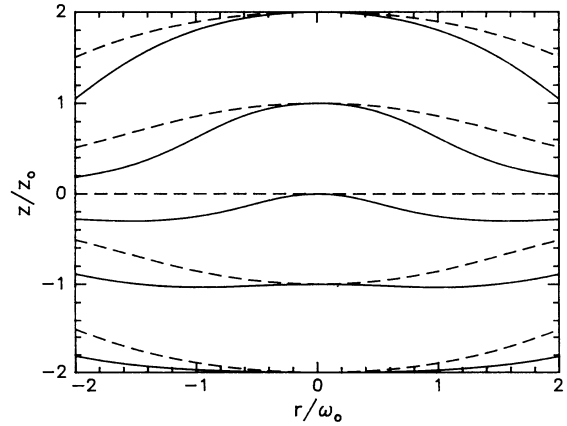

FIG. 3 Same as Fig. 2, except the plot extends over several Rayleigh ranges. Note that the nonorthogonal mode (solid line) has a curvature different from the free-space modes. This is due to gain guiding.

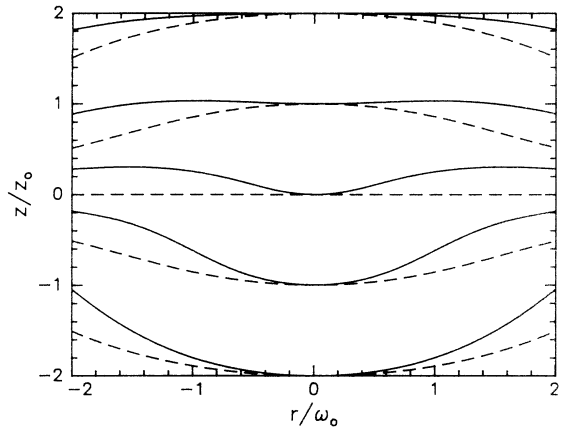

FIG. 4. Wave fronts of lowest-order adjoint mode (solid line) and lowest-order free-space mode (dashed line). To maximize amplifier noise performance, inputs should be constructed as an adjoint mode. The adjoint modes correspond to backward traveling nonorthogonal modes. This can be seen by comparing the solid lines in Fig. 3 to the solid lines in Fig. 4.

wave fronts of $\Phi(z,\mathbf{r}_T)$ over several Rayleigh ranges [18]. For reference, the wave fronts of $U(z,\mathbf{r}_T)$ are also shown. As was the case in the focused region, the wave fronts of the nonorthogonal modes appear to be swept back towards the negative z axis compared to the free-space modes.

As will be discussed in the next section, the adjoint modes play a very important role in optimizing the performance of an amplifier. The relationship between $\Phi(z,\mathbf{r}_T)$ and $\Psi(z,\mathbf{r}_T)$ is such that their transverse intensity distributions are identical. Therefore the solid line in Fig. 1 also represents the adjoint mode profile as well as the nonorthogonal mode profile. However, Fig. 4 shows that the radius of curvature of the adjoint mode differs significantly from the radius of curvature of $\Phi(z,\mathbf{r}_T)$ [18]. Since the adjoint modes correspond to backward propagating nonorthogonal modes there is a symmetry between their respective wave fronts. This can be seen by letting $z\rightarrow -z$ in Fig. 4 and then comparing the plot to Fig. 3; the wave fronts are then identical.

Figures 2–4 were all generated using $G=3$ and a beam waist of $\omega_0=1$ cm. However, for clarity of the plots, the Rayleigh range z_0 was chosen to be 12 cm in Fig. 2 and $\sqrt{2}$ cm in Figs. 3 and 4. The large wavelength $(=\pi\omega_0^2/z_0)$ and the different Rayleigh ranges were chosen only to visually enhance the differences between the various wave fronts shown in Figs. 2–4.

IV. COUPLING

In this section we discuss the performance of a GGA as a function of the input into the amplifier. The SNR is used as a quantitative measure of amplifier performance. To be consistent with quantum mechanics an amplifier must add at least one input noise photon per orthogonal mode [1-3,9–11]. Therefore an amplifier operating at the quantum limit has a SNR of 1 when one photon of signal is input into the amplifier. In the nonorthogonal mode description of a GGA, on the other hand, noise can be transferred among the nonorthogonal modes. As a result, the noise effectively seeding a nonorthogonal mode can be larger than the quantum limit of one photon. Surprisingly this excess noise does not necessarily degrade the SNR of the amplifier. Haus and Kawakami [1] and Siegman [2] have demonstrated that if the input signal is an adjoint mode the SNR would be at the quantum limit. However, to our knowledge no one has studied the SNR of a focused Gaussian GGA for inputs other than an adjoint mode.

The SNR, S/N, for a long, high gain GGA can be calculated by taking the ratio of the first two terms on the right-hand side of Eq. (9). Doing so yields

$$S/N=\frac{\langle\hat{a}^{\dagger}(\theta_i)\hat{a}(\theta_i)\rangle}{B}\ , \tag{10}$$

where the correlation $\langle\hat{a}^{\dagger}(\theta_i)\hat{a}(\theta_i)\rangle$ is proportional to the initial power in the lowest-order nonorthogonal mode $\Phi(\theta,\mathbf{r}_T)$ and B is the overlap integral given in Eq. (5). The SNR depends only on the input into $\Phi(\theta,\mathbf{r}_T)$ because the gain of this mode is much larger than the gain of any other mode. Therefore, even though input into higher-order modes does amplify, the effect of these other modes on the total output power is negligible.

To obtain an expression for the correlation $\langle\hat{a}^{\dagger}(\theta_i)\hat{a}(\theta_i)\rangle$, the input field $\hat{E}^{(-)}(\theta_i,\mathbf{r}_T)$ is written as a linear combination of the nonorthogonal modes [19] $\{\Phi_n^l(\theta,\mathbf{r}_T)\}$,

$$\hat{E}^{(-)}(\theta_i,\mathbf{r}_T)=\left[\frac{2\pi\Delta\nu\hbar\omega}{c}\right]^{1/2}\sum_{n,l}\hat{a}_n^{l\dagger}(\theta_i)\Phi_n^l(\theta_i,\mathbf{r}_T)\ , \tag{11}$$

as in Eq. (3) with $z\rightarrow\theta$. An expression for the lowest-order creation operator $\hat{a}^{\dagger}(\theta_i)$ is found by using the biorthogonality condition given in Eq. (6). The result is

$$\hat{a}^{\dagger}(\theta_i)=\left[\frac{c}{2\pi\Delta\nu\hbar\omega}\right]^{1/2}\int d^2r_T\hat{E}^{(-)}(\theta_i,\mathbf{r}_T)\Psi^{*}(\theta_i,\mathbf{r}_T)\ . \tag{12}$$

When calculating the SNR, the total power of the input signal into the GGA is required to be the same for all of the inputs. We arbitrarily choose the input power to be equal to one photon per unit time such that

$$P=\frac{c}{2\pi}\int d^2r_T\langle\hat{E}^{(-)}(\theta_i,\mathbf{r}_T)\hat{E}^{(+)}(\theta_i,r_T)\rangle=\hbar\omega\Delta\nu\ . \tag{13}$$

Equations (10)–(13) can be used to calculate the SNR for any input into the amplifier. SNR calculations for adjoint mode and nonorthogonal mode inputs are presented to show that the equations describing a GGA with focused Gaussian gain give results which are formally consistent with theories utilizing other gain profiles. In addition, we calculate the SNR for the lowest-order free-space mode (a simple Gaussian). The SNR for a Gaussian mode input is important for experimental reasons. Many optical devices such as single-mode fibers and several types of lasers produce Gaussian beams which

can be input into an amplifier. Nonorthogonal mode inputs are also important experimentally because some experiments make use of consecutive amplifiers [5,10,17,20] in which case the input into the second amplifier is a nonorthogonal mode. The adjoint modes, on the other hand, are more difficult to construct experimentally and therefore have not yet been used as an amplifier input.

First, consider an adjoint mode input such that

$$\hat{E}^{(-)}(\theta_i,\mathbf{r}_T)=\left[\frac{2\pi\Delta\nu\hbar\omega}{c}\right]^{1/2}\hat{b}^{\dagger}(\theta_i)\Psi(\theta_i,\mathbf{r}_T)\ , \quad (14)$$

where $\hat{b}^{\dagger}(\theta_i)$ is the generalized creation operator for the lowest-order adjoint mode. Setting the input power equal to one photon per unit time according to Eq. (13)

$$B\langle\hat{b}^{\dagger}(\theta_i)\hat{b}(\theta_i)\rangle=1\ , \quad (15)$$

where Ref. [14] has also been used. To calculate the SNR using Eq. (10), the adjoint mode creation operator $\hat{b}^{\dagger}(\theta_i)$ must be expressed in terms of the nonorthogonal mode creation operator $\hat{a}^{\dagger}(\theta_i)$. Using Eq. (12), in conjunction with Eq. (14), yields

$$\hat{a}^{\dagger}(\theta_i)=B\hat{b}^{\dagger}(\theta_i)\ . \quad (16)$$

Substituting this expression for $\hat{a}^{\dagger}(\theta_i)$ into Eq. (10) for the SNR and utilizing Eq. (15) gives

$$S/N=1 \text{ (adjoint mode input)} \quad (17)$$

for all values of the gain G. Therefore a GGA can operate at the quantum limit if the input is an adjoint mode.

Since $B>1$, Eq. (16) has a rather peculiar interpretation. Even though the total input power is fixed at one photon per unit time, by configuring the input mode as an adjoint mode it appears that more initial power is deposited in $\Phi(\theta_i,\mathbf{r}_T)$ than if the input itself were one photon per unit time in the mode $\Phi(\theta_i,\mathbf{r}_T)$. Equation (13) still holds, however, because some of the terms in the full expression for output power Eq. (8) are negative. The efficiency of adjoint mode coupling is a consequence of the nonorthogonality of the amplifier modes and points out one of the difficulties of using a nonorthogonal mode basis. Namely, it is not possible to simultaneously specify the number of photons in two distinct nonorthogonal modes [3,13].

Next consider a nonorthogonal mode input into the amplifier. In this case

$$\hat{E}^{(-)}(\theta_i,\mathbf{r}_T)=\left[\frac{2\pi\Delta\nu\hbar\omega}{c}\right]^{1/2}\hat{a}^{\dagger}(\theta_i)\Phi(\theta_i,\mathbf{r}_T)\ . \quad (18)$$

Substituting this into Eq. (13) gives

$$B\langle\hat{a}^{\dagger}(\theta_i)\hat{a}(\theta_i)\rangle=1\ . \quad (19)$$

The SNR is obtained by inserting Eq. (19) into Eq. (10) which gives

$$S/N=1/B^2 \text{ (nonorthogonal mode input)}\ . \quad (20)$$

Therefore amplifier performance is reduced from the quantum limit by precisely the Petermann factor B^2.

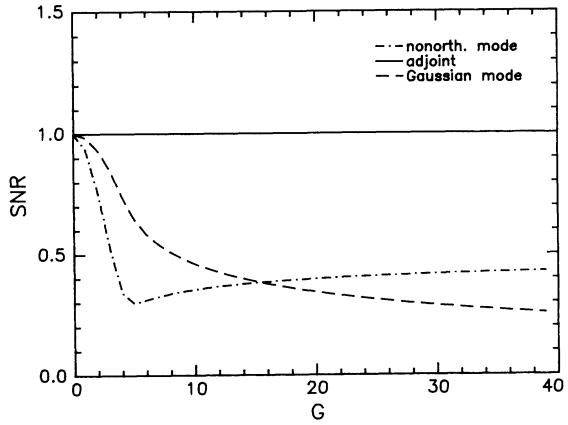

FIG. 5. The signal-to-noise ratio as a function of gain for nonorthogonal mode input, adjoint mode input, and Gaussian mode input. The total input power is the same for each of the three inputs shown. As can be seen, the amplifier couples most strongly to the adjoint mode input. In fact, the amplifier operates at the quantum limit with this input. For the other inputs the SNR is degraded.

Thus the SNR for a nonorthogonal mode input depends on gain. The SNR for this input is plotted (dot-dashed line) as a function of gain in Fig. 5 [21]. At low gains $\Phi(\theta,\mathbf{r}_T)\approx U(\theta,r_T)$; therefore, $B\approx1$ because the free-space modes are orthonormal. In the other extreme, as the gain gets very large $S/N\rightarrow\frac{1}{2}$ as is expected based upon comparison to theories utilizing a two-dimensional parabolic gain profile [1,3]. For intermediate values of the gain, the SNR has a minimum before asymptotically approaching $\frac{1}{2}$. At this point we do not have a complete physical explanation of this phenomena.

The last input to be considered is a Gaussian mode input. The input field is then written

$$\hat{E}^{(-)}(\theta_i,\mathbf{r}_T)=\left[\frac{2\pi\Delta\nu\hbar\omega}{c}\right]^{1/2}\hat{c}^{\dagger}(\theta_i)U(\theta_i,\mathbf{r}_T)\ , \quad (21)$$

where $\hat{c}^{\dagger}(\theta_i)$ is the creation operator for photons in the mode $U(\theta_i,\mathbf{r}_T)$. The input power is normalized by substituting Eq. (21) into Eq. (13), yielding

$$\langle\hat{c}^{\dagger}(\theta_i)\hat{c}(\theta_i)\rangle=1\ . \quad (22)$$

This result is to be expected since the free-space modes constitute an orthonormal set. Equations (12) and (10) then give

$$S/N=\frac{\left|\int d^2r_T U(\theta_i,\mathbf{r}_T)\Psi^{*}(\theta_i,\mathbf{r}_T)\right|^2}{B}$$

$$\text{(Gaussian mode input)}\ . \quad (23)$$

The SNR for a Gaussian input Eq. (23) is plotted as a function of gain (dashed line) in Fig. 5 [21]. Note that the SNR for a Gaussian mode input is a monotonically decreasing function of gain. At low gains $\Psi(\theta_i,\mathbf{r}_T)\approx U(\theta_i,\mathbf{r}_T)$ and the overlap integral in Eq. (23) is large. However, as the gain is increased more and

more free-space modes are needed to form $\Psi(\theta_i,\mathbf{r}_T)$; hence the overlap integral in Eq. (23) steadily decreases.

V. CONCLUSION

We have presented a discussion of the nonorthogonal modes of a GGA with focused Gaussian gain. These modes are found to be narrower (spatially) than the free-space modes due to gain narrowing. They also are found to have a different radius of curvature than the free-space mode as a result of the competition between diffraction and gain narrowing. The SNR for a GGA was found to depend significantly on the shape of the input mode into the amplifier. As discussed by other authors the SNR of the amplifier is found to be at the quantum limit if the input is configured as an adjoint mode, but the SNR is significantly less than the quantum limit if the input is a nonorthogonal mode. We also calculated the SNR for a Gaussian mode input to the amplifier. The SNR is found to be close to the quantum limit at low gains, but decreases steadily as the gain is increased.

ACKNOWLEDGMENT

This work was done under the auspices of National Science Foundation Grant No. PHY-9200104.

APPENDIX

In this appendix Eq. (1) is derived starting from the Maxwell-Bloch equations [12,22] of a gain-guided Raman amplifier. Even though the derivation utilizes equations specific to Raman amplifiers, the result Eq. (1) is general enough to also describe other types of gain-guided amplifiers [2–4]. The starting point for describing growth of the amplified field $\hat{E}^{(-)}(z,\mathbf{r}_T,t)\exp^{i(\omega t-kz)}$ is the Maxwell wave equation [22]

$$\left[\nabla^2-\frac{1}{c^2}\partial_{tt}^2\right]\hat{E}^{(-)}(z,\mathbf{r}_T,t)e^{i(\omega t-kz)} =\frac{2\kappa_2}{c\omega}\partial_{tt}^2[E_L(z,\mathbf{r}_T,t)\hat{Q}^{\dagger}(z,\mathbf{r}_T,t)e^{i(\omega t-kz)}]\ , \quad \text{(A1)}$$

where κ_2 is a coupling constant, c is the velocity of light, $E_L(z,\mathbf{r}_T,t)$ is the (classical) pump laser field which gives the gain profile, and the product $E_L(z,\mathbf{r}_T,t)\hat{Q}^{\dagger}(z,\mathbf{r}_T,t)e^{i(\omega t-kz)}$ is the polarization. In addition, the equation describing the development of the molecular polarization $\hat{Q}^{\dagger}(z,\mathbf{r}_T,t)$ is given by

$$\partial_t\hat{Q}^{\dagger}(z,\mathbf{r}_T,t)=-\Gamma\hat{Q}^{\dagger}(z,\mathbf{r}_T,t) +i\kappa_1E_L^{*}(z,\mathbf{r}_T,t)\hat{E}^{(-)}(z,\mathbf{r}_T,t)+\hat{F}^{\dagger}(z,\mathbf{r}_T,t)\ , \quad \text{(A2)}$$

where Γ is the collisional dephasing rate, κ_1 is another coupling constant, and $\hat{F}^{\dagger}(z,\mathbf{r}_T,t)$ is the Langevin noise operator [12]. Assuming paraxial fields propagating in the z direction, the slowly varying envelope of the amplified electric field $\hat{E}^{(-)}(z,\mathbf{r}_T,t)$ obeys the wave equation [12]

$$(\nabla_T^2-2ik\partial_z)\hat{E}^{(-)}(z,\mathbf{r}_T,\tau)=-2k\kappa_2\hat{Q}^{\dagger}(z,\mathbf{r}_T,\tau)E_L(z,\mathbf{r}_T,\tau) \quad \text{(A3)}$$

where $\tau=t-z/c$ is the retarded time [23].

For times long compared to Γ^{-1}, the polarization approaches a steady-state value. The polarization does fluctuate somewhat due to the Langevin operator, but we assume these fluctuations are small enough such that $\partial_t\hat{Q}^{\dagger}(z,\mathbf{r}_T,t)$ can be set equal to zero in Eq. (A2) [to write Eq. (A2) in the retarded time frame, simply replace each t with a τ]. Roughly, the steady-state approximation is valid if pump laser field is long compared to the time between collisions Γ^{-1}. More rigorously, the approximation is valid if the amplified field grows to its maximum (at a fixed z) in a time long compared to Γ^{-1}. The rate at which the amplified field grows depends on the intensity of the pump laser; therefore the accuracy of the steady-state approximation depends not only on Γ and the pump laser duration, but also on the pump laser intensity [12,22].

Assuming a steady-state polarization, the left-hand side of Eq. (A2) is set equal to zero. The resultant expression for $Q^{\dagger}(z,\mathbf{r}_T,\tau)$ is substituted into Eq. (A3), yielding

$$[\nabla_T^2-2ik\partial_z+ikg(z,\mathbf{r}_T,\tau)]\hat{E}^{(-)}(z,\mathbf{r}_T,\tau) =-4\pi k^2\hat{P}_{\rm sp}^{\dagger}(z,\mathbf{r}_T,\tau) \quad \text{(A4)}$$

where the following definitions have been made:

$$g(z,\mathbf{r}_T,\tau)=\frac{2\kappa_1\kappa_2|E_L(z,\mathbf{r}_T,\tau)|^2}{\Gamma} \quad \text{(A5)}$$

represents the gain profile and

$$\hat{P}_{\rm sp}^{\dagger}(z,\mathbf{r}_T,\tau)=\frac{\kappa_2E_L(z,\mathbf{r}_T,\tau)\hat{F}^{\dagger}(z,\mathbf{r}_T,\tau)}{2\pi k\Gamma} \quad \text{(A6)}$$

is the spontaneous polarization operator. Notice that explicit (slow) time dependence remains in Eq. (A4) even after the steady-state approximation has been made.

Deutsch, Garrison, and Wright [3] have shown, however, that the remaining time dependence can be removed by time averaging Eq. (A4) over the Hertzian bandwidth $\Delta\nu$ of the amplified field according to the rule [3]

$$X(z,\mathbf{r}_T)=\Delta\nu\int_{-1/2\Delta\nu}^{1/2\Delta\nu}d\tau X(z,\mathbf{r}_T,\tau)\ . \quad \text{(A7)}$$

Since we have assumed that the pump field is slowly varying, the gain profile given by Eq. (A5) changes slowly over the time $(\Delta\nu)^{-1}$ so that time averaging the quantity $g(z,\mathbf{r}_T,\tau)\hat{E}^{(-)}(z,\mathbf{r}_T,\tau)$ is straightforward. Averaging the Langevin noise operator in Eq. (A6) over $\Delta\nu$ ensures that only noise frequencies within the bandwidth of $\hat{E}^{(-)}(z,\mathbf{r}_T,\tau)$ will amplify. For the Raman calculations, $\Delta\nu$ is taken to be the gain narrowed Raman linewidth [6]. Applying Eq. (A7) to Eq. (A4) then gives

$$[\nabla_T^2-2ik\partial_z+ikg(z,\mathbf{r}_T)]\hat{E}^{(-)}(z,\mathbf{r}_T)=-4\pi k^2\hat{P}_{\rm sp}^{\dagger}(z,\mathbf{r}_T)\ , \quad \text{(A8)}$$

which is identical to Eq. (1).

[1] H. A. Haus and S. Kawakami, IEEE J. Quantum Electron. **21**, 63 (1985).
[2] A. E. Siegman, Phys. Rev. A **39**, 1253 (1989).
[3] I. H. Deutsch, J. C. Garrison, and E. M. Wright, J. Opt. Soc. Am. B **8**, 1244 (1991).
[4] P. Amendt, R. A. London, and M. Strauss, Phys. Rev. A **44**, 7478 (1991).
[5] S. J. Kuo, D. T. Smithey, and M. G. Raymer, Phys. Rev. **45**, 2031 (1992); Phys. Rev. Lett. **66**, 2605 (1991).
[6] P. R. Battle, J. G. Wessel, and J. L. Carlsten, Phys. Rev. A **48**, 707 (1993); Phys. Rev. Lett. **70**, 1607 (1993).
[7] B. N. Perry, P. Rabinowitz, and M. Newstein, Phys. Rev. A **27**, 1989 (1983).
[8] K. Petermann, IEEE J. Quantum Electron. **15**, 566 (1979).
[9] A. Yariv and S. Magalit, IEEE J. Quantum Electron. **18**, 1831 (1982).
[10] M. D. Duncan, R. Mahon, L. L. Tankersley, and J. Reintjes, J. Opt. Soc. Am. B **9**, 2107 (1992).
[11] P. R. Battle, R. C. Swanson, and J. L. Carlsten, Phys. Rev. A **44**, 1922 (1991).
[12] M. G. Raymer and J. Mostowski, Phys. Rev. A **24**, 1980 (1981).
[13] I. Deutsch, Am. J. Phys. **59**, 834 (1991).
[14] A similar relationship holds for the adjoint modes. It is $B^l_{n,m} = \int d^2 r_T \Psi^{l*}_n(z,\mathbf{r}_T)\Psi^l_m(z,\mathbf{r}_T)$.
[15] For the multiple pass Raman amplifier experiments described in Ref. [6], Eq. (9) is valid for $G > 1$. The relationship between G here and gz in Ref. [6] is $gz = 8.4G$ for the short cell and $gz = 21.0G$ for the long cell.
[16] J. E. LaSala, D. A. G. Deacon, and J. M. J. Madey, Phys. Rev. Lett. **59**, 2047 (1987).
[17] M. D. Duncan, R. Mahon, L. L. Tankersley, and J. Reintjes, J. Opt. Soc. Am. B **7**, 1336 (1990).
[18] The wave fronts shown in Figs. 2–4 are actually wave fronts of total, rapidly varying fields $\exp[-ikz]U(z,\mathbf{r}_T)$, $\exp[-ikz]\Phi(z,\mathbf{r}_T)$, and $\exp[-ikz]\Psi(z,\mathbf{r}_T)$.
[19] Since the nonorthogonal modes do not necessarily form a complete set, there is no guarantee that an arbitrary field can be written as a sum over them. However, we assume that the modes are complete enough to describe the input fields considered here.
[20] D. C MacPherson, R. C. Swanson, and J. L. Carlsten, IEEE J. Quantum Electron. **25**, 1741 (1989).
[21] Although the SNR is shown for arbitrarily small values of G, the plot is only valid when Eq. (9) holds. How large G must be before Eq. (9) holds depends on the experiment. See Ref. [15].
[22] M. G. Raymer, I. A. Walmsley, J. Mostowski, and B. Sobolewska, Phys. Rev. A **32**, 332 (1985).
[23] J. Mostowski and B. Sobolewska, Phys. Rev. A **34**, 3109 (1986).